Shape Optimization of Body Located in Incompressible Navier–Stokes Flow Based on Optimal Control Theory

H. Okumura[1], **M. Kawahara**[1]

Abstract: This paper presents a new approach to a shape optimization problem of a body located in the unsteady incompressible viscous flow field based on an optimal control theory. The optimal state is defined by the reduction of drag and lift forces subjected to the body. The state equation used is the transient incompressible Navier–Stokes equations. The shape optimization problem can be formulated to find out geometrical coordinates of the body to minimize the performance function that is defined to evaluate forces subjected to the body. The fractional step method with the implicit temporal integration and the balancing tensor diffusivity (BTD) formulation are employed for the discretization with the equal–order finite element approximation, while the Crank–Nicolson scheme is used for the temporal discretization. LMQN (Limited-memory quasi–Newton) method, which is an iterative procedure saving the computational memory, is applied for minimizing the performance function. For the numerical study, the optimal shape of the body which has circular shape as the initial state can be finally obtained as the streamlined shape.

keyword: shape optimization, incompressible Navier–Stokes equations, optimal control theory, cyrculaer cylinder, BTD+FS method, LMQN method, finite element method

1 Introduction

The purpose of this paper is to formulate and to solve a shape optimization problem based on an optimal control theory. A formulation concerned with the shape optimization of fluid forces reduction problem of the body located in the incompressible visous flow is presented. The flow can be assumed to be controlled by the geometrical surface coordinates of the body. The optimal state is defined by the reduction of drag and lift forces subjected to the body. The shape optimizaton problem is to find out geometrical surface coordinates of the body to minimize the performance function, which shows the magnitude of the forces. The present performance function consists of integration of a square sum of fluid forces and of a square residual sum between state and initial geometrical coordinates. The state equation acts as constraint condition of the performance funciton. The state equation is expressed as the transient incompressible Navier–Sokes equations. The Lagrange multiplier method is applied to the constraint condition of the performance function and a Lagrange multiplier equation is obtained. This equation is equivalent to the adjoint operator of a linealized version of the state equation, which is referred to as the adjont equation. The equation is dependent on the state equation and has to be solved backwards in time, starting from a final condition called the transversality condition. It is convenient to obtain the gradient of the performance funciton with respect to the geometrical surface coordinates, introducing an efficient method for the minimization of the performance function.

The fractional step method [Hayashi, Hatanaka and Kawahara (1991)] with the implicit temporal integration and the balancing tensor diffusivity (BTD) formulation [Gresho, Chan, Lee and Upson (1984)] called the *BTD+FS* method are employed in this paper for the discretization with the equal–order finite element approximation. The Limited–memory quasi–Newton (LMQN) method [Zou, Navon, Berger and Phua (1993)] with the L–BFGS invese Hessian updating formula, which is an iterative procedure saving the computational memory, is applied to the minimization algorithm of the performance funciton. This algorithm is easy to implement and its convergence rate is stable. As a numerical example, the present shape optimization method is applied to the fluid force reduction problem of a circular cylider located in the viscous flow at Reynolds number $Re = 200$. Computed results for optimized case are displayed with the inital state. An efficient idea for dealing with the transversality condition of the adjoint equations for the shape optimization problem is also proposed.

2 State Equations

Let Ω denote the spatial domain representing $\boldsymbol{x}$ the coordinates associated with Ω at the time $t \in (0, T)$. Let Γ denote the boundary of Ω supposing that the incompressible viscous fluid flow, which occupies Ω. The state equation of the flow can be written by the following incompressible Navier–Stokes equation in the non–dimensional form:

$$\frac{\partial \boldsymbol{u}}{\partial t} + \boldsymbol{u}\cdot\nabla\boldsymbol{u} + \nabla p - \nabla\cdot\left\{\nu\left[\nabla\boldsymbol{u} + (\nabla\boldsymbol{u})^T\right]\right\} = \boldsymbol{0} \quad \text{in } \Omega\times(0,T), \tag{1}$$

$$\nabla\cdot\boldsymbol{u} = 0 \quad \text{in } \Omega\times(0,T), \tag{2}$$

where, $\boldsymbol{u}$ and p are velocity and pressure, ν is inverse of the Reynolds number ($\nu = 1/Re$), respcetively.

[1] Department of Civil Engineering, Chuo University; Kasuga 1-13-27, Bunkyo-ku, Tokyo 112-8551, Japan.

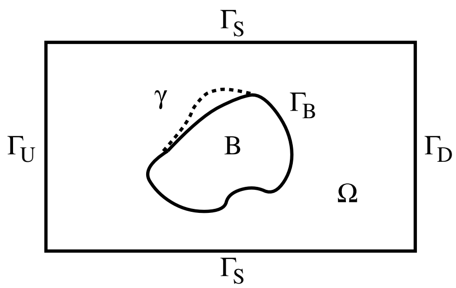

Figure 1 : Analytical domain and boudary conditions

Consider a typical problem described in Fig. 1, in which a solid body of cross–section B with the boundary Γ_B is laid in the external flow. Suppose that the boundary of Ω is denoted by $\Gamma = \Gamma_U \cup \Gamma_D \cup \Gamma_S \cup \Gamma_B$. The boundary of B is also assumed to be included for the boundary of optimal shape that can control fluid force on $\gamma \subset \Gamma_B$ by the movable surface. The boundary condition and divergence–free initial condition for this problem are given as:

$$\boldsymbol{u} = (U, 0) \quad \text{on } \Gamma_U \times (0,T), \tag{3}$$

$$\boldsymbol{t} = \left\{-p\boldsymbol{I} + \nu\left[\nabla\boldsymbol{u} + (\nabla\boldsymbol{u})^T\right]\right\} \cdot \boldsymbol{n} = \boldsymbol{0} \quad \text{on } \Gamma_D \times (0,T), \tag{4}$$

$$t_1 = 0,\ u_2 = 0 \quad \text{on } \Gamma_S \times (0,T), \tag{5}$$

$$\boldsymbol{u} = \boldsymbol{0} \quad \text{on } \Gamma_B \cup \gamma \times (0,T), \tag{6}$$

$$\boldsymbol{u}(\boldsymbol{x}, 0) = \boldsymbol{u}_0 \ (\text{with } \nabla \cdot \boldsymbol{u}_0 = 0) \quad \text{in } \Omega_0, \tag{7}$$

where U is constant inflow velocity, $\boldsymbol{t}$ is traction vector, $\boldsymbol{I}$ is identity tensor, $\boldsymbol{n}$ is unit vector of outward normal to Γ, respectively.

The fluid forces acted on the cylinder B are denoted by (D, L), where D and L are drag and lift forces, respectively. The fluid forces (D, L) are obtained by integrating the traction $\boldsymbol{t}$ on Γ_B.

$$(D, L) = -\int_{\Gamma_B} \boldsymbol{t}\, \mathrm{d}\Gamma \tag{8}$$

3 Formulation for Shape Optimization

The shape optimization problem can be formulated using an optimal contorl strategy. In case of optimal control problem with constraint condition, the performance function should be minimized satisfying the state equation. This problem can be transformed into the minimization problem without constraint condition by the Lagrangian multiplier or the adjoint equation using adjoint variable for state variable of the state equation.

3.1 Performance Function

The shape optimization problem is formulated by the optimal control theory in which a performance function is defined and geometrical suface coordinates $\boldsymbol{x}_c$ of the body is found to minimize the performance function. Abergel and Temam pointed out that for the optimal control problem of the Navier–Stokes equation, the performance function can be formulated using the square sum of velocity itself, energy dissipation and curl of velocty [Abergel and Temam (1990)]. In this paper, a fluid force control problem is considered, thus, the fluid force is directly used in the performance function. The performance function $J(\boldsymbol{x}_c)$ is defined by the temporal integration of a square sum of fluid forces and of square residual sum between state geometrical coordinate $\boldsymbol{x}_c$ and referrence geometrical coordinates $\boldsymbol{x}^*$ from time $t = 0$ to $t = T$.

$$J(\boldsymbol{x}_c) = \frac{1}{2}\int_0^T (q_1 D^2 + q_2 L^2)\mathrm{d}t + \frac{1}{2}\int_0^T \int_\gamma r(\boldsymbol{x}_c - \boldsymbol{x}^*)^2\, \mathrm{d}\Gamma\, \mathrm{d}t \tag{9}$$

where q_1, q_2 and r are the weighting parameters, and it is noted that the the state vector is denoted by $\boldsymbol{x}_c$ and referrence surface coordinates of the body is $\boldsymbol{x}^*$.

The state equations (1) and (2) are the constraint conditions of the performance function $J(\boldsymbol{x}_c)$. The Lagrange multiplier method is suitable for the optimal control problem with the constraint conditions. The Lagrange multipliers for the state equations (1) and (2) are defined as the adjoint velocity $\boldsymbol{y}$ and adjoint pressure λ. The temporal integration of a dot product between adjoint velocity $\boldsymbol{y}$ and pressure λ and state equations (1) and (2) is added to the performance function $J(\boldsymbol{x}_c)$, the extended performance function $J^*(\boldsymbol{x}_c)$ can be obtained as follows:

$$\begin{aligned} J^*(\boldsymbol{x}_c) = {} & \frac{1}{2}\int_0^T (q_1 D^2 + q_2 L^2)\mathrm{d}t + \frac{1}{2}\int_0^T \int_\gamma r(\boldsymbol{x}_c - \boldsymbol{x}^*)^2\, \mathrm{d}\Gamma\, \mathrm{d}t \\ & - \int_0^T \int_\Omega \boldsymbol{y} \cdot \{\frac{\partial \boldsymbol{u}}{\partial t} + \boldsymbol{u} \cdot \nabla\boldsymbol{u} + \nabla p - \nabla \cdot \{\nu[\nabla\boldsymbol{u} + (\nabla\boldsymbol{u})^T]\}\}\mathrm{d}\Omega\, \mathrm{d}t \\ & + \int_0^T \int_\Omega \lambda \nabla \cdot \boldsymbol{u}\, \mathrm{d}\Omega\, \mathrm{d}t \end{aligned} \tag{10}$$

If the state equations (1) and (2) are satisfied, the third and fourth terms can be zero. The essence of the performance function $J(\boldsymbol{x}_c)$ does not change with the addition of the extended performance function $J^*(\boldsymbol{x}_c)$.

3.2 Derivation of Adjoint Equation

To minimize the performance function $J(\boldsymbol{x}_c)$, the gradient of the performance function $J(\boldsymbol{x}_c)$ with respect to goemetrical surface coordinatess $\boldsymbol{x}_c$ should be introduced. The optimal control problem with the constraint condition of the state equations (1) and (2) results in solving a stationary condition of the extended performance function $J^*(\boldsymbol{x}_c)$ instead of the original performance function $J(\boldsymbol{x}_c)$. The necessary condition for the stationary condition is that the first variation of the extended performance funciton $J^*(\boldsymbol{x}_c)$ vanish. The first–order necessary condition for the optimality condition is derived from the first variation of the extended performance function $J^*(\boldsymbol{x}_c)$,

$$\delta J^*(\boldsymbol{x}_c) = 0. \tag{11}$$

Taking an integration by parts for each necessary term, the first variation of the performance function $J(\boldsymbol{x}_c)$ yields as follows:

$$\begin{aligned}
\delta J^*(\boldsymbol{x}_c) &= \delta \boldsymbol{u}\frac{\partial J(\boldsymbol{x}_c)}{\partial \boldsymbol{u}} + \delta p\frac{\partial J(\boldsymbol{x}_c)}{\partial p} + \delta \boldsymbol{y}\frac{\partial J(\boldsymbol{x}_c)}{\partial \boldsymbol{y}} \\
&+ \delta\lambda\frac{\partial J(\boldsymbol{x}_c)}{\partial \lambda} + \delta \boldsymbol{x}_c\frac{\partial J(\boldsymbol{x}_c)}{\partial \boldsymbol{x}_c} \\
&= -\int_0^T\int_\Omega \delta\boldsymbol{u}\cdot\{-\frac{\partial \boldsymbol{y}}{\partial t} + (\nabla\boldsymbol{u})^T\boldsymbol{y} - (\boldsymbol{u}\cdot\nabla)\boldsymbol{y} \\
&+ \nabla\lambda - \nabla\cdot\{\nu[\nabla\boldsymbol{y} + (\nabla\boldsymbol{y})^T]\}\}\,\mathrm{d}\Omega\,\mathrm{d}t \\
&+ \int_0^T\int_\Omega \delta p\nabla\cdot\boldsymbol{y}\mathrm{d}\Omega\mathrm{d}t + \int_0^T\int_{\Gamma_U}\delta\boldsymbol{t}\cdot\boldsymbol{y}\mathrm{d}\Gamma\,\mathrm{d}t \\
&+ \int_0^T\int_{\Gamma_S}\delta t_2\, y_s\,\mathrm{d}\Gamma\,\mathrm{d}t \\
&+ \int_0^T\int_{\Gamma_B}\{\delta t_1(y_1 - q_1 D) + \delta t_2(y_2 - q2L)\}\mathrm{d}\Gamma\mathrm{d}t \\
&- \int_0^T\int_{\Gamma_D}\delta\boldsymbol{u}\cdot\boldsymbol{s}\mathrm{d}\Gamma\,\mathrm{d}t - \int_0^T\int_{\Gamma_S}\delta u_1\, s_1\,\mathrm{d}\Gamma\,\mathrm{d}t \\
&- \int_0^T\int_\gamma \delta\boldsymbol{x}_c\cdot\{(\nabla\boldsymbol{u})^T\boldsymbol{s} - r(\boldsymbol{x}_c - \boldsymbol{x}^*)\}\,\mathrm{d}\Gamma\,\mathrm{d}t \\
&- \int_\Omega \delta\boldsymbol{u}(\boldsymbol{x},T)\cdot\boldsymbol{y}(\boldsymbol{x},T)\mathrm{d}\Omega = 0, \qquad (12)
\end{aligned}$$

where $\boldsymbol{s}$ is,

$$\boldsymbol{s} = \{\boldsymbol{u}\boldsymbol{y} - \lambda\boldsymbol{I} + \nu[\nabla\boldsymbol{y} + (\nabla\boldsymbol{y})^T]\}\cdot\boldsymbol{n} \qquad (13)$$

and the following relation is used:

$$\begin{aligned}
&\int_0^T(\delta D\, q_1 D + \delta L\, q_2 L)\mathrm{d}t \\
&= -\int_0^T(\delta\int_{\Gamma_B} t_1\mathrm{d}\Gamma\, q_1 D + \delta\int_{\Gamma_B} t_2\mathrm{d}\Gamma\, q_2 L)\mathrm{d}t \\
&= -\int_0^T\int_{\Gamma_B}(\delta t_1\, q_1 D + \delta t_2\, q_2 L)\mathrm{d}\Gamma\,\mathrm{d}t. \qquad (14)
\end{aligned}$$

Setting each term equal to zero to satisfy the optimality contidition, the following adjoint equation, adjoint boundary conditions and terminal condition can be obtained, respectively:

$$-\frac{\partial \boldsymbol{y}}{\partial t} + (\nabla\boldsymbol{u})^T\boldsymbol{y} - \boldsymbol{u}\cdot\nabla\boldsymbol{y} + \nabla\lambda - \nabla\cdot\{\nu\left[\nabla\boldsymbol{y} + (\nabla\boldsymbol{y})^T\right]\} = \boldsymbol{0} \quad \text{in } \Omega\times(0,T), \qquad (15)$$

$$\nabla\cdot\boldsymbol{y} = 0 \quad \text{in } \Omega\times(0,T), \qquad (16)$$

$$\boldsymbol{y} = \boldsymbol{0} \quad \text{on } \Gamma_U\times(0,T), \qquad (17)$$

$$\boldsymbol{s} = \boldsymbol{0} \quad \text{on } \Gamma_D\times(0,T), \qquad (18)$$

$$s_1 = 0,\ y_2 = 0 \quad \text{on } \Gamma_S\times(0,T), \qquad (19)$$

$$\boldsymbol{y} = (q_1 D, q_2 L) \quad \text{on } \Gamma_B\cup\gamma\times(0,T), \qquad (20)$$

$$\boldsymbol{y}(\boldsymbol{x},T) = \boldsymbol{0} \quad \text{in } \Omega. \qquad (21)$$

Solving state and adjoint equations, the gradient of performance function $J(\boldsymbol{x}_c)$ with respect to geometrical surface coordinates $\boldsymbol{x}_c$ is calculated by the following equation:

$$\delta\boldsymbol{x}_c\frac{\partial J(\boldsymbol{x}_c)}{\partial \boldsymbol{x}_c} = \int_0^T\int_\gamma \delta\boldsymbol{x}_c\cdot\{(\nabla\boldsymbol{u})^T\boldsymbol{s} - r(\boldsymbol{x}_c - \boldsymbol{x}^*)\}\mathrm{d}\Gamma\,\mathrm{d}t. \qquad (22)$$

Let $\boldsymbol{x}_c$ be the optimal solution, then the following equality holds,

$$(\nabla\boldsymbol{u})^T\boldsymbol{s} - r(\boldsymbol{x}_c - \boldsymbol{x}^*) = \boldsymbol{0} \quad \text{on } \gamma\times(0,T). \qquad (23)$$

4 Discretization

4.1 Performance Function and Its Gradient

The discretization of the boundary γ and geometrical surface coordinates $\boldsymbol{x}_c$ of the body is defined as M connected components γ_m and geometric surface coordinates $\boldsymbol{x}_{c(m)}$,

$$\gamma = \bigcup_{m=1}^{M}\gamma_m, \qquad (24)$$

$$\forall m = 1,2,\cdots,M, \qquad \boldsymbol{x}_c = \boldsymbol{x}_{c(m)} \qquad \text{on} \quad \gamma_m\times(0,T) \qquad (25)$$

The total number of time steps is denoted by N and the time increment is by $\Delta t = T/N$, where T is the total computational time. The performance function (9) and its gradient (22) can be discretized as:

$$\begin{aligned}
J_{\Delta t}(\boldsymbol{x}_{c(m)}^{(n)}) &= \frac{1}{2}\sum_{n=1}^{N}(q_1 D^{(n)2} + q_2 L^{(n)2})\Delta t \\
&+ \frac{1}{2}\sum_{n=1}^{N}\sum_{m=1}^{M}\int_{\gamma_m} r(\boldsymbol{x}_{c(m)}^{(n)} - \boldsymbol{x}_{(m)}^{*(n)})^2\mathrm{d}\Gamma\Delta t, \qquad (26)
\end{aligned}$$

$$\begin{aligned}
&\delta(\boldsymbol{x}_{c(m)}^{(n)})\frac{\partial J_{\Delta t}(\boldsymbol{x}_{c(m)}^{(n)})}{\partial \boldsymbol{x}_{c(m)}^{(n)}} = \\
&\int_{\gamma_m}\delta\boldsymbol{x}_{c(m)}^{(n)}\cdot\{(\nabla\boldsymbol{u}^{(n)})^T\boldsymbol{s}^{(n)} - r(\boldsymbol{x}_{c(m)}^{(n)} - \boldsymbol{x}_{(m)}^{*(n)})\}\mathrm{d}\Gamma\Delta t \qquad (27)
\end{aligned}$$

4.2 Governing Equation

The Crank–Nicholson method is applied to momentum equation (1), for the temporal discretization:

$$\frac{\boldsymbol{u}^{n+1} - \boldsymbol{u}^n}{\Delta t} + \boldsymbol{u}^n\cdot\nabla\boldsymbol{u}^{n+\frac{1}{2}} + \nabla p^{n+1} - \nu\nabla^2\boldsymbol{u}^{n+\frac{1}{2}} = \boldsymbol{0} \quad \text{in} \quad \Omega\times(0,T), \qquad (28)$$

$$\nabla\cdot\boldsymbol{u}^{n+1} = 0 \qquad \text{in} \quad \Omega\times(0,T), \qquad (29)$$

where $\boldsymbol{u}^{n+\frac{1}{2}}$ denotes $(\boldsymbol{u}^n + \boldsymbol{u}^{n+1})/2$, and the advection velocity in the non–linear term is approximated by the known velocity $\boldsymbol{u}^n$.

The BTD+FS method [Hayashi, Hatanaka and Kawahara (1991)][Gresho, Chan Lee and Upson (1984)] is employed for momentum equation (28) and continuity equation (29). The approximated functions of the weighting and trial functions for the velocity and pressure are denoted by $\boldsymbol{w}_h$, q_h,$\boldsymbol{u}_h$ and p_h, respectively. The bi– or trilinear interpolation function is used for $\boldsymbol{w}_h$, q_h,$\boldsymbol{u}_h$ and p_h in this paper. The weighting residual equations can be obtained as:

$$\int_\Omega q_h \nabla \cdot \boldsymbol{u}_h^n \, \mathrm{d}\Omega + \int_\Omega \Delta t \nabla q_h \cdot \{\boldsymbol{u}_h^n \cdot \nabla \boldsymbol{u}_h^n + \nabla p_h^{n+1} - \nu \nabla^2 \boldsymbol{u}_h^n\} \, \mathrm{d}\Omega = 0, \tag{30}$$

$$\int_\Omega \boldsymbol{w}_h \cdot \{\frac{\boldsymbol{u}_h^{n+1} - \boldsymbol{u}_h^n}{\Delta t} + \boldsymbol{u}_h^n \cdot \nabla \boldsymbol{u}_h^{n+\frac{1}{2}}\} \mathrm{d}\Omega + \int_\Omega \nabla \boldsymbol{w}_h : \{-p_h^{n+1}\boldsymbol{I} + \nu \nabla^2 \boldsymbol{u}_h^{n+\frac{1}{2}}\} \mathrm{d}\Omega + \int_\Omega \frac{\Delta t}{2} \boldsymbol{u}_h^n \cdot \nabla \boldsymbol{w}_h \cdot \{\frac{\boldsymbol{u}_h^{n+1} - \boldsymbol{u}_h^n}{\Delta t} + \boldsymbol{u}_h^n \cdot \nabla \boldsymbol{u}_h^{n+\frac{1}{2}} + \nabla p_h^{n+1} - \nu \nabla^2 \boldsymbol{u}_h^{n+\frac{1}{2}}\} \mathrm{d}\Omega = \boldsymbol{0}, \tag{31}$$

In equation (30), to increase a computational efficiency, the unknown velocity $\boldsymbol{u}^{n+\frac{1}{2}}$ is approximated by the known velocity $\boldsymbol{u}^n$.

4.3 Adjoint Equation

The Crank–Nicholson method is also applied to adjoint momentum equation (15), and the adjoint continuity equation (16) is also treated as the full implicit scheme for the temporal discretization:

$$\frac{\boldsymbol{y}^{n-1} - \boldsymbol{y}^n}{\Delta t} + (\nabla \boldsymbol{u}^n)^T \boldsymbol{y} - \boldsymbol{u}^n \cdot \nabla \boldsymbol{y}^{n-\frac{1}{2}} - \nabla \lambda^{n-1} - \nu \nabla^2 \boldsymbol{y}^{n-\frac{1}{2}} = \boldsymbol{0} \quad \text{in} \quad \Omega \times (0, T), \tag{32}$$

$$\nabla \cdot \boldsymbol{y}^{n-1} = 0 \quad \text{in} \quad \Omega \times (0, T), \tag{33}$$

where $\boldsymbol{y}^{n-\frac{1}{2}}$ denotes $(\boldsymbol{y}^n + \boldsymbol{y}^{n-1})/2$.

The BTD+FS method is employed for adjoint momentum (32) and adjoint continuity (33) equations. The approximated functions of weighting and trial functions for velocity and pressure are denoted by $\boldsymbol{w}_h$, θ_h,$\boldsymbol{y}_h$ and λ_h, respectively. The bi– or trilinear interpolation function is used for $\boldsymbol{w}_h$, θ_h,$\boldsymbol{y}_h$ and θ_h in this paper. The weighting residual equation can be obtained as:

$$\int_\Omega \theta_h \nabla \cdot \boldsymbol{y}_h^n \, \mathrm{d}\Omega - \int_\Omega \Delta t \nabla \theta_h \cdot \{(\nabla \boldsymbol{u}_h^n)^T \boldsymbol{y} - \int_\Omega \Delta t \nabla \theta_h \cdot -\boldsymbol{u}_h^n \cdot \nabla \boldsymbol{y}_h^n + \nabla \lambda_h^{n+1} - \nu \nabla^2 \boldsymbol{y}_h^n\} \, \mathrm{d}\Omega = 0, \tag{34}$$

$$\int_{\Omega_n} \boldsymbol{w}_h \cdot \{\frac{\boldsymbol{y}_h^{n-1} - \boldsymbol{y}_h^n}{\Delta t} + (\nabla \boldsymbol{u}_h^n)^T \boldsymbol{y}_h^n\} \mathrm{d}\Omega + \int_{\Omega_n} \nabla \boldsymbol{w}_h : \{\boldsymbol{u}_h^n \boldsymbol{y}_h^{n-\frac{1}{2}} - \lambda_h^{n-1}\boldsymbol{I} + \nu \nabla^2 \boldsymbol{y}_h^{n-\frac{1}{2}}\} \mathrm{d}\Omega - \int_{\Omega_n} \frac{\Delta t}{2} \boldsymbol{u}_h^n \cdot \nabla \boldsymbol{w}_h \cdot \{\frac{\boldsymbol{y}_h^{n-1} - \boldsymbol{y}_h^n}{\Delta t} + (\nabla \boldsymbol{u}_h^n)^T \boldsymbol{y}_h^n - \boldsymbol{u}_h^n \cdot \nabla \boldsymbol{y}_h^{n-\frac{1}{2}} + \nabla \lambda_h^{n-1} - \nu \nabla^2 \boldsymbol{y}_h^{n-\frac{1}{2}}\} \mathrm{d}\Omega = \boldsymbol{0}, \tag{35}$$

In equation (34), to increase a computational efficiency, the unknown velocity $\boldsymbol{y}^{n-\frac{1}{2}}$ is approximated by the known velocity $\boldsymbol{y}^n$.

5 Minimization Algorithm

Limited–memory quasi–Newton (LMQN) mehtod [Zou, Navon Berger and Phua (1993)] is applied for the minimization algorithm. The advantage of this mehtod is applicable for large–scale problem because of the modest storage requirements using a sparse approximation to the Hessian matrix. The Limited–memory BFGS (L–BFGS) method is used for updating the approximation of the inverse Hessian matrix.

Consider a problem of finding a control vector $\boldsymbol{v}$ to minimize the performance function $J(\boldsymbol{v})$, the algorithm of the LMQN method is given as follows:

1. Chose an initial $\boldsymbol{v}$ and a positive definite initial approximation to the inverse matrix $\bar{m}H_0$, which may be chosen as the identity matrix.
2. Compute
$$\boldsymbol{G}_0 = \frac{\partial J(\boldsymbol{v}_0)}{\partial \boldsymbol{v}}. \tag{36}$$
and set
$$\boldsymbol{d}_0 = -\boldsymbol{H}_0 \boldsymbol{G}_0. \tag{37}$$
3. For $k = 0, 1, \ldots$ set
$$\boldsymbol{v}_{k+1} = \boldsymbol{v}_k + \alpha_k \boldsymbol{d}_k \tag{38}$$
where α_k is the step size that is obtained by the linear search.
4. Compute
$$\boldsymbol{G}_{k+1} = \frac{\partial J(\boldsymbol{v}_{k+1})}{\partial \boldsymbol{v}}. \tag{39}$$
5. Generate a new search direction $\boldsymbol{d}_{k+1}$ by setting.
$$\boldsymbol{d}_{k+1} = -\boldsymbol{H}_{k+1} \boldsymbol{G}_{k+1}. \tag{40}$$
6. Check for convergence: If
$$||\boldsymbol{G}_{k+1}|| \le \varepsilon ||\boldsymbol{v}_{k+1}|| \tag{41}$$
then stop where ε is a positive small allowance, otherwise continue from step 3.

For the linear search, a rough linear search method is used. the width of search α_k can be given as the following equation.

$$J(\boldsymbol{v}_k + \alpha_k \boldsymbol{d}_k) \le J(\boldsymbol{v}_k) + 0.0001\, \alpha_k \boldsymbol{G}_k^t \boldsymbol{d}_k \tag{42}$$

$$|\frac{\boldsymbol{G}(\boldsymbol{v}_k + \alpha_k \boldsymbol{d}_k)^t \boldsymbol{d}_k}{\boldsymbol{G}_k^t \boldsymbol{d}_k}| \le 0.9 \tag{43}$$

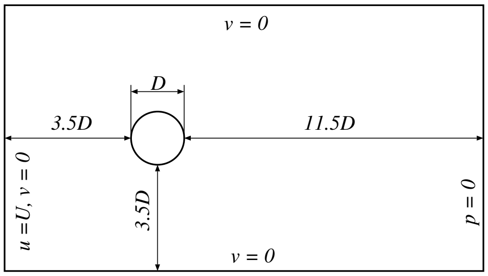

Figure 2 : Analytical domain

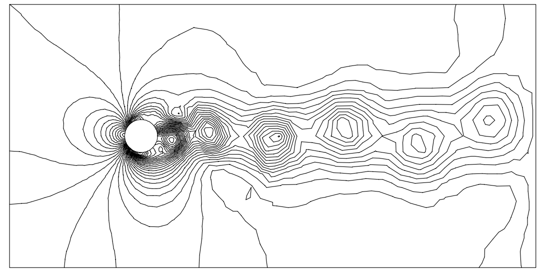

Figure 5 : Iso–pressure contours

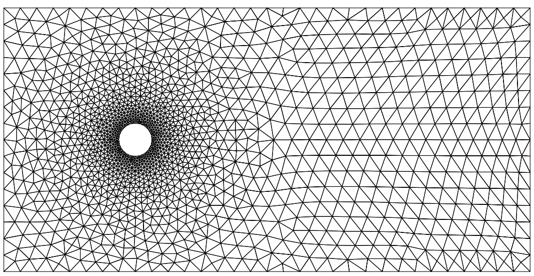

Figure 3 : Finite element mesh

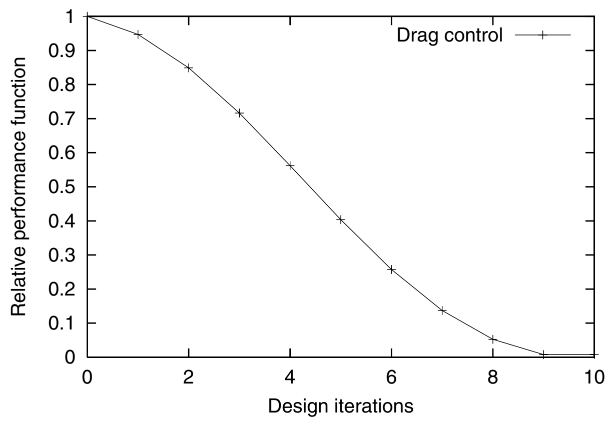

Figure 6 : Number of iterations versus performance funciton

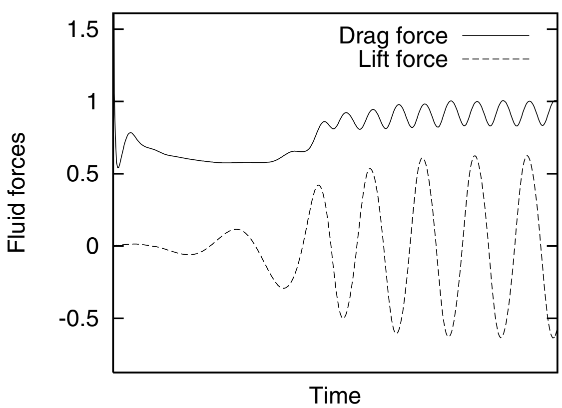

Figure 4 : Time history of fluid forces

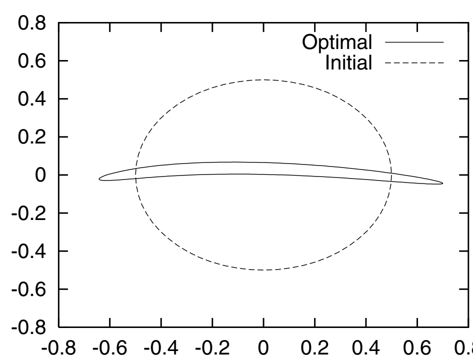

Figure 7 : Initial and optimal shape

The renewal of the inverse of Hessian matrix can be given by the following L–BFGS formula. In the L–BFGS formula, the inverse of Hessian matrix can be given by $\boldsymbol{v}$ and $\boldsymbol{G}$ at last m_{th} iteration.

$$\begin{aligned}\boldsymbol{H}_{k+1} &= (\boldsymbol{w}_k^t \cdots \boldsymbol{w}_{k-\hat{m}}^t)\boldsymbol{H}_0\,(\boldsymbol{w}_{k-\hat{m}} \cdots \boldsymbol{w}_k) \\ &+ \rho_{k-\hat{m}}\,(\boldsymbol{w}_k^t \cdots \boldsymbol{w}_{k-\hat{m}+1}^t)\,\boldsymbol{p}_{k-\hat{m}}\boldsymbol{p}_{k-\hat{m}}\,(\boldsymbol{w}_{k-\hat{m}+1} \cdots \boldsymbol{w}_k) \\ &+ \rho_{k-\hat{m}+1}\,(\boldsymbol{w}_k^t \cdots \boldsymbol{w}_{k-\hat{m}+2}^t)\,\boldsymbol{p}_{k-\hat{m}+1}\boldsymbol{p}_{k-\hat{m}+1} \\ &(\boldsymbol{w}_{k-\hat{m}+2} \cdots \boldsymbol{w}_k) + \cdots + \boldsymbol{p}_k\boldsymbol{p}_k \end{aligned} \tag{44}$$

where, $\boldsymbol{p}_k = \boldsymbol{v}_{k+1} - \boldsymbol{v}_k$, $\boldsymbol{q}_k = \boldsymbol{G}_{k+1} - \boldsymbol{G}_k$, $\rho_k = 1/(\boldsymbol{q}_k^t \boldsymbol{p}_k)$, $\boldsymbol{w}_k$ is $\boldsymbol{w}_k = \boldsymbol{I} - \rho_k \boldsymbol{q}_k \boldsymbol{p}_k^t$. And $\boldsymbol{I}$ is a unit matrix.

6 Numerical Example

For numerical examples, the present shape optimization method is applied to fluid force reduction problem of a circular cylinder located in the viscous flow. Fig. 2 and 3 show the domain used for the present analysis and finite element mesh. The number of control boundary γ_m is $M = 60$. The domain $\Omega \setminus \bar{B}$ is $(-4, 4) \times (-4, 12)$ and B is the disk of center $(0, 0)$ and of radius 0.5. The total number of time steps is $N = 800$,

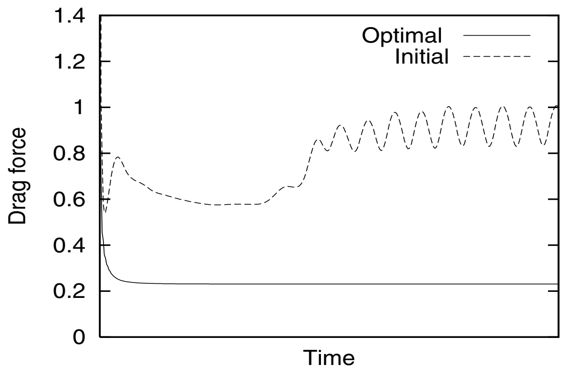

Figure 8 : Time history of drag force

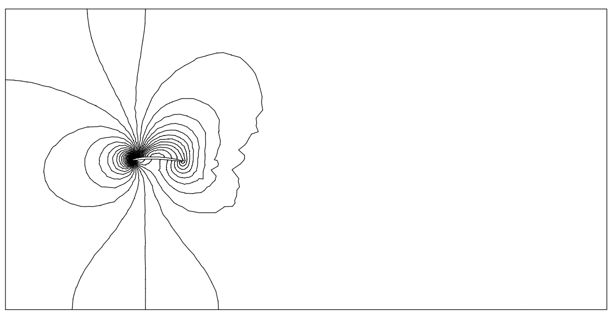

Figure 9 : Iso–pressure contours (optimal)

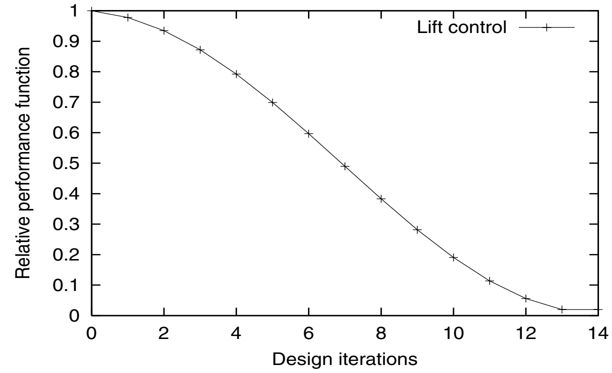

Figure 10 : Number of iterations versus performance funciton

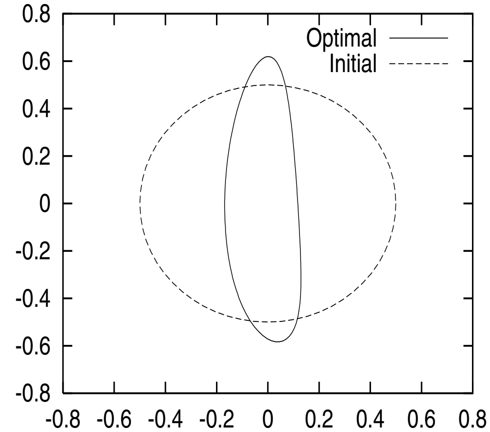

Figure 11 : Initial and optimal shape

and the time increment is $\Delta t = 0.05$, thus the terminal time is $T = 40$. The Reynolds number based on tye cylinder diameter and inflow velocity is $Re = 200$ ($\nu = 0.005$). Fig. 4 shows time history of fluid forces. Fig. 5 shows iso–pressure contours ($t = 40$). Allowance ε is 10^{-5}.

6.1 Drag Force Reduction Problem

The purpose of the present is reduce the drag force, while the lift force and the circular cilinder volume are not kept unchanged in this case. The weighting parameters are chosen as $q_1 = 1, q_2 = 0, r = 1$. Thus, this control problem is only drag force reduction. Fig. 6 shows the number of iterations versus the relative performance funciton J. It is observed that the reduction of the performance function is achived and 10 iterations need to be converged. It is seen that the amplitude of the drag force is reduced. For this numecical example, the optimal shape of the body which has circular shape as the initial state can be finally obtained as the streamlined shape like a wing shown in Fig. 7. For the drag force to be redueced, the optimal shape has been obtained as flat configuration. However the initial shape has a smooth edge. This means that the precent shape optimization method has to be able to treat the apparition of signular points. No particluar treatment such as a Spline interpolation has been done for this case. The initial drag force should be positive as the flow direction is uniform. This means that the optimal shape is ansymmetric. Fig. 8 shows the time history of the drag force D. Iso–pressure contours in optimal ($t = 40$) is shown in Fig. 9.

6.2 Lift Force Reduction Problem

This control problem is only lift force reduction, thus The weighting parameters are $q_1 = 0, q_2 = 1, r = 1$, thus, Fig. 10 shows the number of iterations versus the relative performance funciton J. It is observed that the reduction of the performance function is achived and 14 iterations need to be converged. It is seen that the amplitude of the lift force is reduced. For this numecical example, the optimal shape of the body which has circular shape as the initial state can be finally obtained as shown in Fig. 11. This shape is the streamlined one like a wing. The initial lift force should be periodic as the initial shape is symmetric. The optimal shape is almost symmetric. Fig. 12 shows the time history of the drag force L. Iso–pressure contours in optimal ($t = 40$) is shown in Fig. 13.

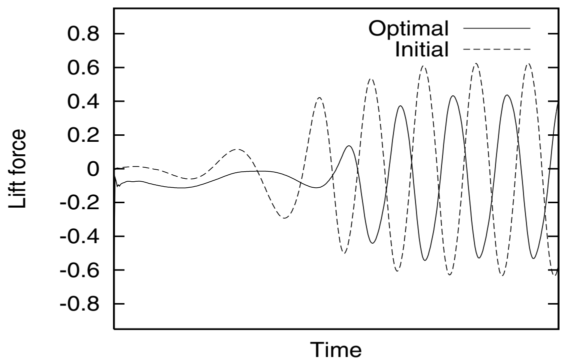

Figure 12 : Time history of lift force

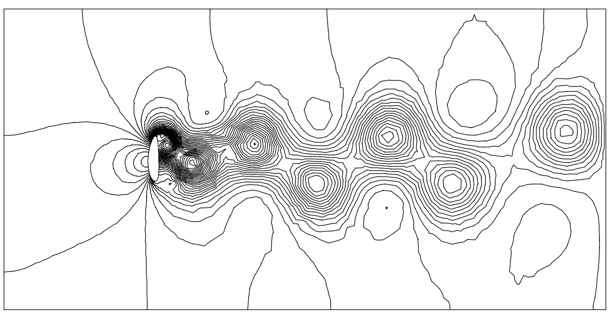

Figure 13 : Iso–pressure contours (optimal)

7 Conclusion

A formulation for shape optimization of the incompressible Navier–Stokes equations has been presented in this paper. The BTD+FS method has been used for the spatial discretization, while the Crank–Nicolson scheme was used for the temporal discretization. The LMQN (Limited–memory quasi–Newton) method has been applied as the mimization technique. A computational method of optimal shape design for the body located in the transient incompressible viscous fluid flow has been presented to feature a new shape optimization approach based on the optimal control theory. As a numerical example, fluid force reduction problem of a circuler cylinder located in the the present shape optimization method is applied to fluid force reduction problem of a circular cylider located in the viscous flow at Reynolds number $Re = 200$. The modified transversality condition that is the solution of the steady Lagrange multiplier equation has been proposed. The shape optimization is presented in this peper successful, and it is confirmed that the present shape optmization method is very effective and robust to implement for the incompressible Navier–Stokes equations. Future work will include to expand this technique in three–dimensional configuratins.

References

Hayashi, M.; Hatanaka, K.; and Kawahara, M.(1991): Lagrangian finite element method for free surface Navier–Stokes flow using fractional step methods, *Int. J. Num. Meth. FLuids*, Vol.13, pp.805–840

Gresho, P. M.; Chan, S. T.; Lee, R. L. and Upson, C. D.(1984): A modified finite element method for the solving the time–dependent incompressible Navier-Stokes equations, Part 1 & 2, *J. Meth. Fluid*, Vol.4, pp.557–598 & pp.619–640.

Zou, X.; Navon, I. M.; Berger, M. and Phua, K. H.(1993): Numerical Experience with Limited–Memery Quasi–Newton and Trancated Newton Methods, *Siam J. Optimization*, Vol.3, pp. 582–608.

Abergel, F.; Temman, R.(1990): On some Control Problems in Fluid Mechanics, *Thecoret. Comput. Fluid Dynamics*, Vol.1, pp. 303–325.